Indian Journal of Biochemistry & Biophysics
Vol. 63, September 2026, pp. 1099-1111
DOI: 10.56042/ijbb.v63i9.22771

Synthesis of imidazole derivatives and *in silico*/*in vitro* evaluation of potential antidiabetic activity

Sanjana Mareguddi[1], Prabitha Prabhakaran[2], Ammar Abdul Razzak Mahmood[3], Saleem Javid[4], Nina Bhagyanath[5] & Somashekar Mahadevappa Metri[1]*

[1]Department of Pharmaceutical Chemistry, BLDEA's Shri Sanganabasava Mahaswamiji College of Pharmacy and Research Centre, Vijayapur-586 103, Karnataka, India

[2]Department of Pharmaceutical Chemistry, JSS College of Pharmacy, JSS Academy of Higher Education & Research, Mysuru-570 010, Karnataka, India

[3]Department of Pharmaceutical Chemistry, College of Pharmacy, University of Baghdad, Baghdad, Iraq

[4]Yenepoya Pharmacy College and Research Centre, Yenepoya (Deemed to be University) University Road, Deralakatte, Mangalore-575 018, Karnataka, India

[5]Department of Pharmaceutical Chemistry, Al-Ameen College of Pharmacy, Bangalore-560 027, Karnataka, India

Received 15 August 2025; *revised 16 July 2026*

Diabetes mellitus (DM) is a chronic metabolic disorder characterized by persistent hyperglycemia due to insulin resistance or deficiency. The imidazole scaffold, a privileged heterocycle in medicinal chemistry, has shown significant promise in targeting key enzymes involved in type 2 DM (T2DM). In this study, eight novel imidazole derivatives were designed, synthesized, and structurally characterized using ^{1}H NMR, ^{13}C NMR, and mass spectrometry. Molecular docking studies against α-amylase and α-glucosidase revealed favourable binding affinities (−7.2 to −8.8 kcal/mol) and strong interactions with key catalytic residues. ADMET predictions using ADMET Lab 3.0 and SwissADME indicated good drug-likeness for most derivatives, and the top docking hit was subjected to a 100 ns molecular dynamics simulation (Desmond), which confirmed complex stability with minimal RMSD fluctuations (~1.8 Å) and persistent hydrogen bonding. *In vitro* α-amylase inhibition assays demonstrated potent activity, with compound SM-04 exhibiting an IC_{50} of 21.5 ± 1.2 µM, comparable to the reference drug acarbose (18.9 ± 1.4 µM). MTT assays on 3T3-L1 cells indicated low cytotoxicity for all compounds. Overall, the synthesized imidazole derivatives displayed promising *in silico* and *in vitro* antidiabetic potential, supporting their development as leads for T2DM therapy.

Keywords: α-Amylase inhibition, Dacarbazine, Imidazole derivatives, Ketoconazole, Losartan

Diabetes mellitus (DM) is a chronic metabolic disorder that has emerged as a major global health concern. As of 2021, more than 537 million adults are living with diabetes worldwide, and this number is projected to escalate to 643 million by 2030 and 783 million by 2045[1,2]. This sharp rise is attributed to factors such as sedentary lifestyles, unhealthy dietary habits, obesity, aging populations, and genetic predisposition. DM is primarily characterized by persistent hyperglycemia resulting from defects in insulin secretion, insulin action, or both. Prolonged hyperglycemia leads to progressive damage to various organ systems and is associated with serious complications, including nephropathy, retinopathy, neuropathy, and cardiovascular diseases, which contribute significantly to morbidity, mortality, and healthcare costs[3]. Type 2 diabetes mellitus (T2DM) represents 90–95% of all DM cases and is mainly driven by insulin resistance and progressive pancreatic β-cell dysfunction[4].

Despite the availability of several pharmacotherapeutic options, current treatments often fall short due to adverse effects, limited efficacy in halting disease progression, and poor patient compliance[5]. This highlights an urgent need for the development of safer, multi-targeted therapeutic agents that can address the multifactorial nature of T2DM. In this context, heterocyclic compounds, particularly nitrogen-containing heterocycles, have attracted significant attention in drug discovery due to their diverse pharmacological activities and structural versatility[6].

*Correspondence:
Phone: +91-9972087801 (Mob)
E-mail: ssmcop.somashekharmetri@bldea.org; csm.som@gmail.com

Suppl. data available on respective page of NOPR

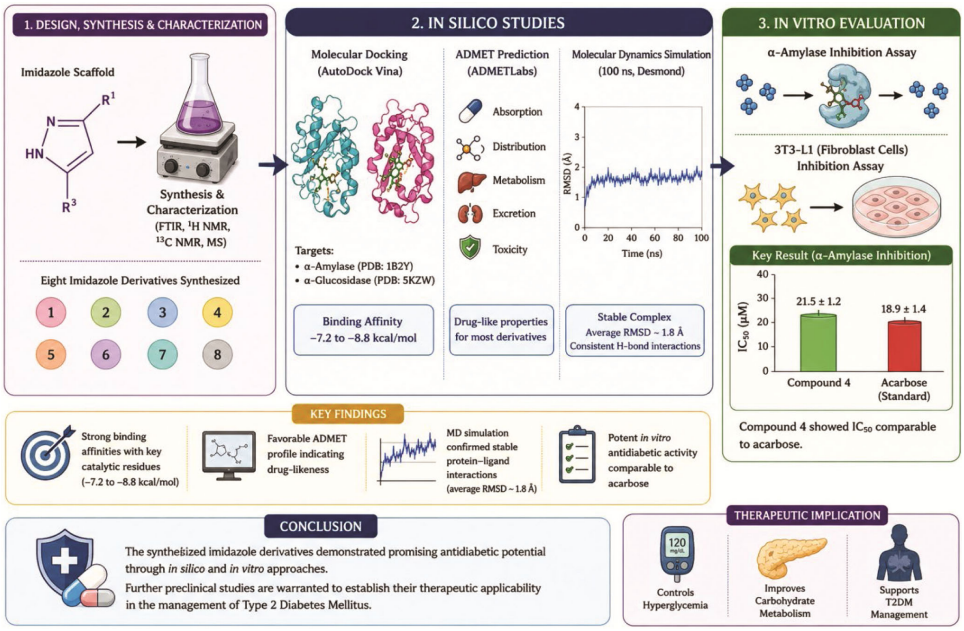

Graphical abstract

Among these, the imidazole ring system stands out as a privileged scaffold, present in numerous clinically approved drugs, including antifungals (*e.g.*, ketoconazole), antihypertensives (*e.g.*, losartan), and anticancer agents (*e.g.*, dacarbazine)[7,8]. More recently, imidazole derivatives have shown promising antidiabetic activity, attributed to their ability to inhibit key carbohydrate-hydrolyzing enzymes such as α-amylase and α-glucosidase, as well as their potential to modulate the activity of peroxisome proliferator-activated receptor gamma (PPAR-γ). These mechanisms are particularly relevant in managing postprandial hyperglycemia and improving insulin sensitivity[9,10].

Advancements in computer-aided drug design (CADD) tools have significantly streamlined early-stage drug discovery. Techniques such as molecular docking and ADMET (absorption, distribution, metabolism, excretion, and toxicity) profiling enable the rapid screening of compounds with favourable pharmacokinetic and pharmacodynamic properties[11,12]. However, molecular docking provides only a static representation of protein–ligand interactions. To gain deeper insights into the stability and dynamic behavior of these complexes under physiological conditions, molecular dynamics (MD) simulations are employed, offering a more realistic understanding of binding efficacy and conformational flexibility[13].

Nonetheless, computational predictions must be complemented by experimental validation to ensure biological relevance. *In vitro* enzyme inhibition assays targeting α-amylase and α-glucosidase serve as a widely accepted approach to evaluate the antidiabetic potential of novel compounds[14].

Considering this, the present study was designed to synthesize and evaluate eight novel imidazole derivatives as potential antidiabetic agents. An integrative research strategy was adopted, encompassing molecular docking to predict binding affinity to diabetic targets, ADMET profiling to assess drug-likeness, MD simulations to evaluate complex stability, and *in vitro* assays to confirm inhibitory activity against α-amylase and α-glucosidase. This comprehensive approach aims to provide valuable insights into the design and development of new therapeutic candidates for the effective management of T2DM.

Material and Methods

Chemicals and Reagents

All chemicals and reagents used in the study were of analytical grade and procured from Molychem (India) and Sigma-Aldrich (USA). Solvents were purified before use according to standard protocols. The progress and purity of the synthesized compounds were monitored by thin-layer chromatography (TLC) using silica gel G-coated plates (Merck), and the spots were visualized under ultraviolet (UV) light.

Melting points were determined using a Precision Melting Point Apparatus in open capillary tubes and are reported uncorrected. Fourier-transform infrared

(FT-IR) spectra were recorded on a SHIMADZU spectrophotometer, and the characteristic absorption frequencies are expressed in cm^{-1} (ν_{max}). Proton (^1H) and carbon (^{13}C) nuclear magnetic resonance (NMR) spectra were acquired on a Bruker 400 MHz NMR spectrometer using $CDCl_3$ as the solvent and tetramethylsilane (TMS) as the internal standard. Mass spectra were recorded using a Waters Micromass ZQ instrument via the direct injection method.

General procedure for the synthesis of imidazole derivatives

Synthesis of 2-(4-methoxyphenyl)-4,5-diphenyl-1H-imidazole (2)

A mixture of benzil (25 mmol), 4-methoxybenzaldehyde (25 mmol), and ammonium acetate (130 mmol) was dissolved in glacial acetic acid (100 mL) and refluxed under magnetic stirring for 1 h. Upon completion, the reaction mixture was allowed to cool to room temperature and then diluted with distilled water (500 mL). The resulting precipitate was collected by vacuum filtration. The filtrate was subsequently neutralized with aqueous ammonium hydroxide (NH_4OH), resulting in the formation of an additional solid, which was also collected by filtration. Both solid fractions were combined and recrystallized from aqueous ethanol to afford pure 2-(4-methoxyphenyl)-4,5-diphenyl-1H-imidazole as a white crystalline solid in 86% yield (melting point: 213–214°C)[15].

Synthesis of 2-chloro-1-[2-(4-methoxyphenyl)-4,5-diphenyl-1H-imidazol-1-yl] ethan-1-one (3)

A solution of 2-(4-methoxyphenyl)-4,5-diphenyl-1H-imidazole (0.01 mol) in acetone (20 mL) was prepared and stirred, followed by the addition of anhydrous potassium carbonate (K_2CO_3, 0.02 mol). Chloroacetyl chloride (0.01 mol) was then added dropwise via a dropping funnel while maintaining the reaction at a low temperature. The reaction mixture was stirred for 5–6 h under these conditions. Upon completion, the solvent was removed under reduced pressure, and the resulting residue was washed with 5% aqueous sodium bicarbonate solution and cold distilled water. The crude product was dried and recrystallized from ethanol to afford 2-chloro-1-[2-(4-methoxyphenyl)-4,5-diphenyl-1H-imidazol-1-yl]ethan-1-one as a white crystalline solid (93% yield; m.p. 200–202°C)[15].

Synthesis of 2-hydrazineyl-1-(2-(4-methoxyphenyl)-4,5-diphenyl-1H-imidazol-1-yl) ethan-1-one (SM)

2-chloro-1-[2-(4-methoxyphenyl)-4,5-diphenyl-1H-imidazol-1-yl] ethan-1-one (6 g, 0.01 mol) was refluxed in ethanol (50 mL) with hydrazine hydrate (99%, 1.94 mL, 0.03 mol) for 12 h. After completion of the reaction, the mixture was allowed to cool to room temperature, resulting in the formation of a solid precipitate. The product was collected by filtration, washed thoroughly with distilled water, dried under vacuum, and recrystallized from aqueous ethanol to afford the corresponding hydrazide derivative as a white crystalline solid (86% yield; melting point: 220–223°C)[16].

Synthesis of Aromatic Halide Derivatives (SM-01 to SM-08)

A solution of 2-hydrazinyl-1-[2-(4-methoxyphenyl)-4,5-diphenyl-1H-imidazol-1-yl] ethan-1-one (0.03 mol) and the corresponding aromatic halide (0.03 mol) in ethanol (30 mL) was refluxed in the presence of potassium hydroxide (KOH, 0.39 g). The progress of the reaction was monitored by thin-layer chromatography (TLC) at 2 h intervals. Upon completion, the reaction mixture was allowed to cool and was left to stand overnight at room temperature. The resulting solid was collected, dried under vacuum, and recrystallized from aqueous ethanol to afford the desired aryl-substituted hydrazone derivatives as pure crystalline solids[16] (Fig. 1).

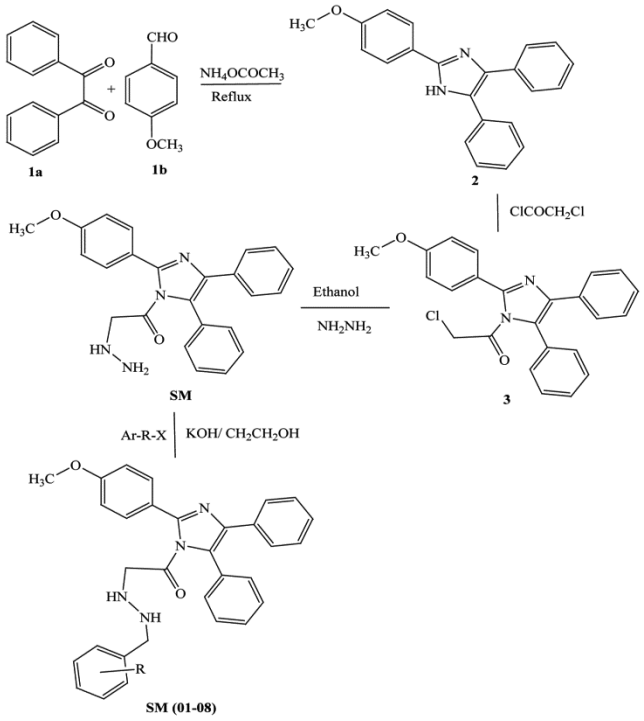

Fig. 1— Scheme for Synthesis of Imidazole Derivatives (SM-01 to SM-08)

***In silico*validation**

Molecular docking and ADMET analysis

Molecular docking studies were carried out using AutoDock Vina v1.5.7 to investigate the binding interactions of the synthesized imidazole derivatives (SM-01 to SM-08) with human pancreatic α-amylase (PDB ID: 1B2Y)[17] and human acid α-glucosidase (GAA) (PDB ID: 5KZW). Two-dimensional chemical structures of the ligands were drawn using ChemDraw Ultra and converted into energy-minimized three-dimensional conformations with Open Babel. The crystal structures of the target enzymes were validated using ProSA, ERRAT, and Ramachandran plot analyses to confirm structural reliability before docking.

For docking preparation, all water molecules were removed, polar hydrogens were added, and Kollman charges were assigned to the receptor proteins. Docking was performed using default parameters, and binding poses were analysed for interactions with key catalytic residues[18].

Molecular dynamics

Molecular dynamics (MD) simulations were performed using Desmond with the OPLS_2005 force field to evaluate the dynamic stability of the top-ranked docked complexes of SM-04 with human pancreatic α-amylase (PDB ID: 1B2Y) and human acid α-glucosidase (PDB ID: 5KZW). Each protein–ligand complex was solvated in an orthorhombic box using the TIP3P water model, maintaining a buffer distance of 10 Å from the protein surface. The systems were neutralized by adding appropriate counterions and 0.15 M NaCl to mimic physiological conditions.

Energy minimization was performed before equilibration, which was carried out under the NPT ensemble (constant number of particles, pressure, and temperature) at 300 K and 1 atm, using the MartynaTobias–Klein barostat and the Nose–Hoover thermostat. Production runs were conducted for 100 ns with a time step of 2 fs. Periodic boundary conditions were applied in all directions, and long-range electrostatics were calculated using the Particle Mesh Ewald (PME) method[19].

Trajectory data were recorded every 100 ps for post-simulation analysis, including root mean square deviation (RMSD), root mean square fluctuation (RMSF), hydrogen bond occupancy, and protein–ligand interaction profiles[20].

Absorption, Distribution, Metabolism, Excretion, and Toxicity (ADMET) studies

in silico pharmacokinetic and toxicity predictions were performed using SwissADME, ADMETlab 3.0, and ProTox, providing ADMET profiles, as well as drug-likeness parameters for all compounds[21].

***In vitro* study**

MTT assay for Cytotoxicity and Protective effect

The cytotoxic and protective activities of the synthesized compounds (SM-01 to SM-08) against glucose-induced oxidative stress were determined in 3T3-L1 fibroblast cells using the MTT [3-(4,5-dimethylthiazol-2-yl)-2,5-diphenyltetrazolium bromide] assay (Table 1). Cells were seeded into 96-well plates at a density of 1×10^4 cells per well and maintained under standard culture conditions (37°C, 5% CO_2, humidified atmosphere) until they reached approximately 70% confluence.

Hyperglycemic stress was induced by treating cells with D-glucose (200 mg/dL) for 24 h. The test compounds were applied at final concentrations of 20, 40, 60, 80, and 100 µg/mL. Following treatment, MTT solution (5 mg/mL in PBS) was added to each well, and the plates were incubated for 4 h at 37°C.

Table 1— Binding affinity and interaction of synthesised compound and standard drug acarbose with proteins 1B2Y and 5KZW

S. No.	Ligands	Binding Affinity (kcal/mol)	Vander waals	Binding Affinity (kcal/mol)	Vander waals
			PDBID: 1B2Y		PDBID: 5KZW
1	Acarbose	-8.7	ALA 198, GLY 164, HIS 299	-9.6	GLU 474, PRO 475
2	SM-01	-7.6	LEU 162, THR 163, TRP 357	-8.6	HIS 717, PRO 198ASO 356
3	SM-02	-7.6	LEU 162, TRP 357, THR 163, GLY 306	-8.8	GLY 359, ARG 585
4	SM-03	-7.6	TRP 59, TRP 357, THR 163, GLY 306	-8.0	SER 676, TRP 481
5	SM-04	-7.3	TRP 59, TRP 357VAL 354	-8.8	GLY 359, TYR 609
6	SM-05	-7.6	TRP 357, GLY 304, THR 163	-8.6	PHE 525, LEU 283
7	SM-06	-7.7	TRP 357, GLY 304 THR163	-8.8	GLY 359, LEU 355
8	SM-07	-7.4	TRP 59, VAL 354	-8.7	GLY 359, ASP 356
9	SM-08	-7.7	TRP 357, GLY 306 THR163	-8.8	ARG 229, LEU 231

The medium was removed, and dimethyl sulfoxide (DMSO) was used to solubilize the formazan crystals formed.

Absorbance was measured at 550 nm using a microplate reader, and the percentage of viable cells was calculated relative to the untreated control group[22].

α-amylase enzyme inhibition assay

The *in vitro* α-amylase inhibitory potential of the synthesized compounds (SM-01 to SM-08) was assessed using a modified Bernfeld protocol. Test samples were prepared in phosphate buffer (pH 6.9) to obtain final concentrations of 20, 40, 60, 80, and 100 µg/mL. To each concentration, α-amylase solution (0.5 mg/mL in phosphate buffer) was added, and the mixture was pre-incubated at 37°C for 10 min.

Enzymatic reactions were initiated by introducing 1% (*w/v*) soluble starch in phosphate buffer as the substrate, followed by incubation at 37°C for another 10 min. The reaction was stopped by adding dinitrosalicylic acid (DNSA) reagent and subsequently heating the mixture in a boiling water bath for 5 min to develop color. After cooling to ambient temperature, absorbance was recorded at 540 nm using a microplate reader. Blank and control samples were processed in parallel, and the percentage inhibition was calculated with respect to the enzyme control[23].

Statistical analysis

The α-amylase inhibition activity was expressed as mean ± SD of triplicate experiments, and IC_{50} values were determined by nonlinear regression analysis of percent inhibition versus log inhibitor concentration using Excell 2019.

Results

Experimental data

All synthesized derivatives (SM-01 to SM-08) were characterized by determining melting points, Rf values, ^{1}H NMR, ^{13}C NMR, and mass spectrometry. The results confirmed the structures of the target compounds. All the interpreted data are in the supplementary file.

Molecular docking analysis

All ligands (SM-01 to SM-08) and the reference inhibitor acarbose were docked against α-glucosidase (PDB ID: 1B2Y) and α-amylase (PDB ID: 5KZW). The docking scores ranged from −7.3 to −7.7 kcal/mol for α-glucosidase and −8.0 to −8.8 kcal/mol for α-amylase, with acarbose showing the strongest binding (−8.7 and −9.6 kcal/mol, respectively). Among the test compounds, SM-06 and SM-08 achieved the best scores against α-glucosidase (−7.7 kcal/mol), while SM-02, SM-04, SM-06, and SM-08 exhibited the strongest α-amylase inhibition (−8.8 kcal/mol). Key van der Waals contacts involved conserved catalytic and binding site residues, notably TRP357, THR163, and GLY306 in α-glucosidase, and GLY359, ARG585, and TYR609 in α-amylase (Figs. 2-5).

ADMET prediction

All synthesized compounds (SM-01 to SM-08) exhibited favorable ADMET profiles with high predicted gastrointestinal (GI) absorption (except SM-06) and no predicted blood–brain barrier (BBB) penetration. LogP values ranged from 5.68 to 6.98, indicating high lipophilicity compared to acarbose (–8.56). All compounds showed moderate to good predicted bioavailability scores (0.17–0.55) and minimal hepatotoxicity/nephrotoxicity risks (Table 2).

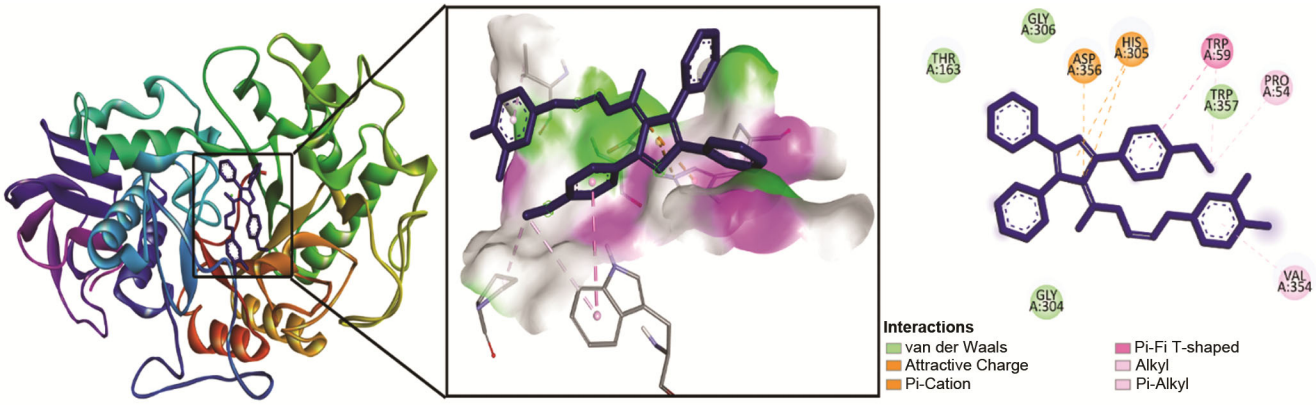

Fig. 2 — 2D & 3D Interaction between ligand SM-06 & protein 1B2Y

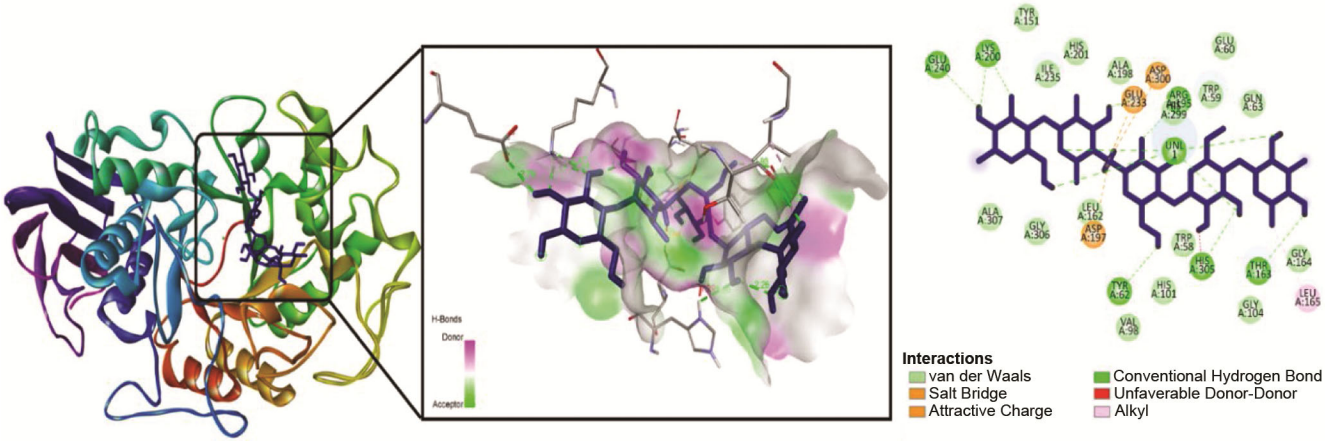

Fig. 3 — 2D & 3D Interaction between ligand Acarbose & protein 1B2Y

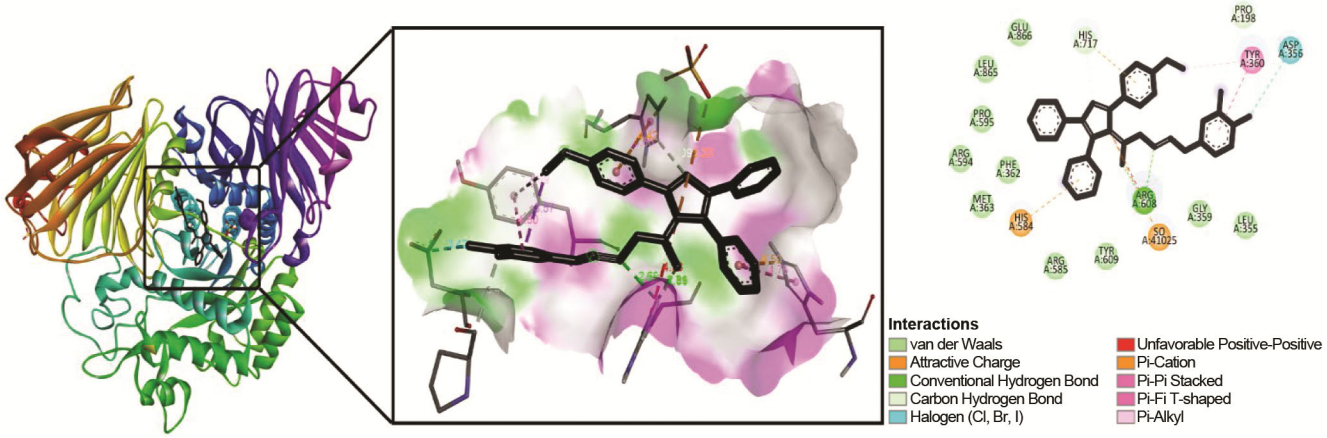

Fig. 4 — 2D & 3D Interaction between ligand SM-06 & protein 5KZW

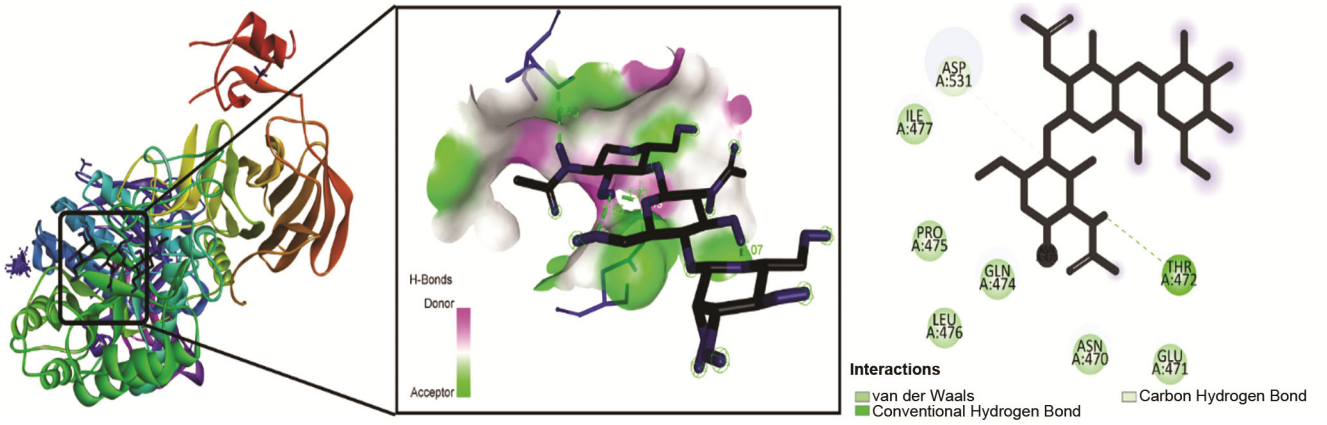

Fig. 5 — 2D & 3D Interaction between ligand Acarbose & protein 5KZW

MD simulation

Molecular dynamics simulations were carried out for the top-ranked docked complex, SM-04 with α-amylase (PDB ID: 1B2Y) and α-glucosidase (PDB ID: 5KZW). The RMSD analysis of the SM-04 complexes demonstrated stable protein–ligand interactions throughout the 100 ns simulation period (Fig. 6). For the SM-04_1B2Y complex (left), the protein RMSD stabilized around 1.2–1.4 Å after ~10 ns, indicating minimal conformational deviation from the initial structure, while the ligand RMSD rapidly stabilized within the first 10 ns at ~9.8–10.5 Å, suggesting early and sustained accommodation within the binding pocket. In the SM-04_5KZW complex

Table 2— ADMET analysis of the synthesised compound (SM01-08) and Acarbose

SI No	Compound Code	MW	H D	H A	logP	BBB	GI	Bioavalability	Hepatotoxicity	Nephrotoxicity
1	Acarbose	645.2	14	19	8.56	No	Low	0.17	0.65	0.8
2	SM-01	488.8	2	5	5.68	No	High	0.55	0.57	0.50
3	SM-02	488.8	2	5	5.68	No	High	0.55	0.57	0.50
4	SM-03	523	2	5	6.33	No	High	0.17	0.55	0.50
5	SM-04	523	2	5	6.33	No	High	0.17	0.55	0.50
6	SM-05	502.6	2	5	5.98	No	High	0.17	0.57	0.51
7	SM-06	557.6	2	5	6.98	No	Low	0.17	0.55	0.50
8	SM-07	514.6	2	5	6.21	No	High	0.17	0.58	0.51
9	SM-08	567.4	2	5	6.44	No	High	0.17	0.56	0.51

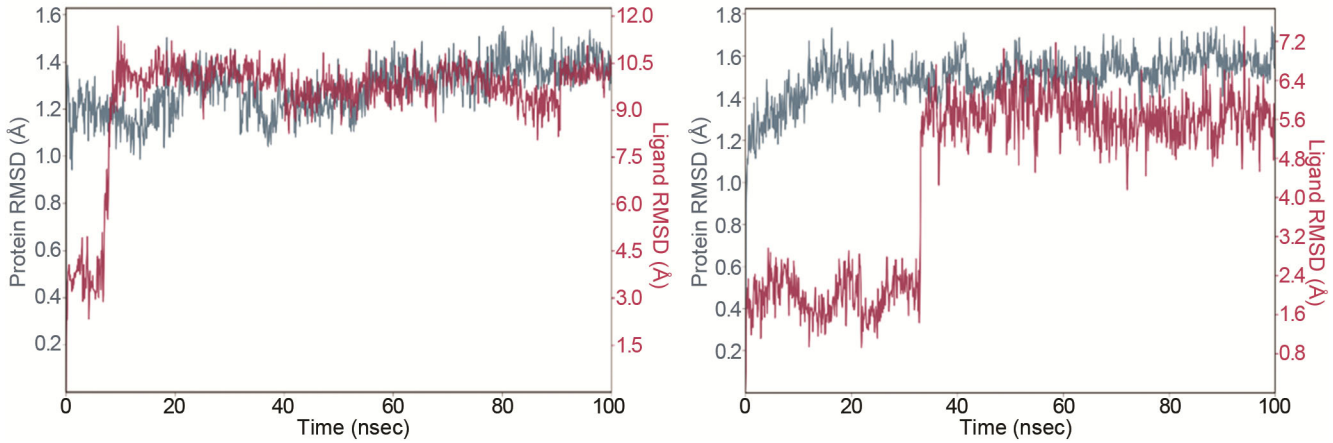

Fig. 6 — RMSD plots of SM-04_1B2Y complex (left) & SM-04_5KZW complex (right)

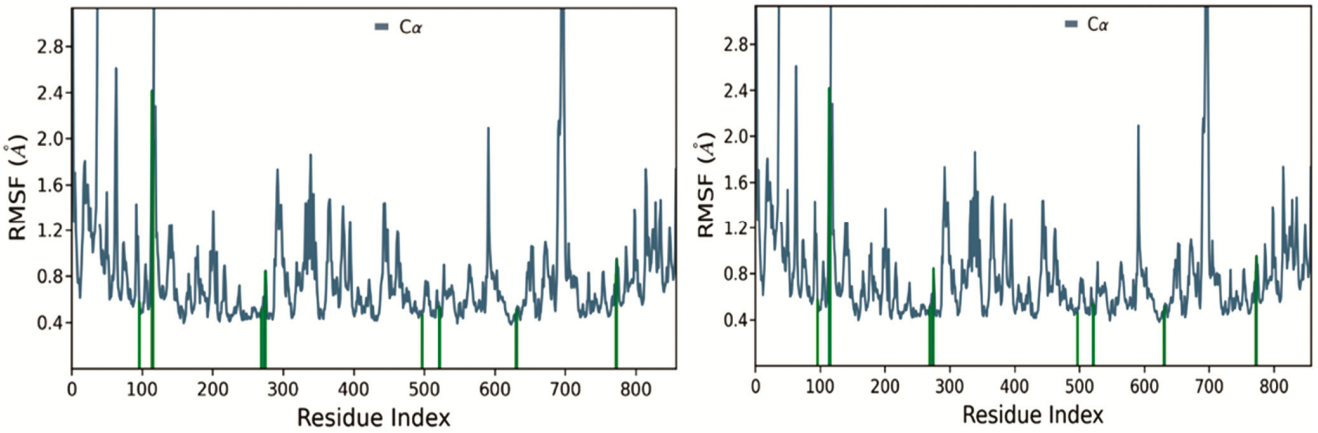

Fig. 7 — RMSF plots of protein 1B2Y (left) & protein 5KZW (right) highlighting protein flexibility across the 100 ns simulation

(right), the protein RMSD remained consistent at ~1.4–1.6 Å after ~15 ns, with the ligand RMSD showing a marked shift around 40 ns, stabilizing thereafter at ~5.8–6.4 Å. These stable RMSD profiles for both protein and ligand across the simulations confirm the conformational stability of SM-04 in both α-glucosidase and α-amylase active sites, supporting its predicted high-affinity binding.

Both systems displayed stable ligand RMSD values, consistent radius of gyration, and minimal fluctuations in solvent-accessible surface area (SASA) and polar surface area (PSA). Molecular surface area (MolSA) remained within the expected range, indicating no significant structural collapse. Hydrogen bonding interactions were maintained throughout the trajectory, confirming stable ligand–protein associations (Figs. 6-9, and Table 3).The RMSF analysis of the SM-04–protein complexes (Fig. 7) revealed overall low backbone flexibility, indicating stable protein structures during the 100 nsMD

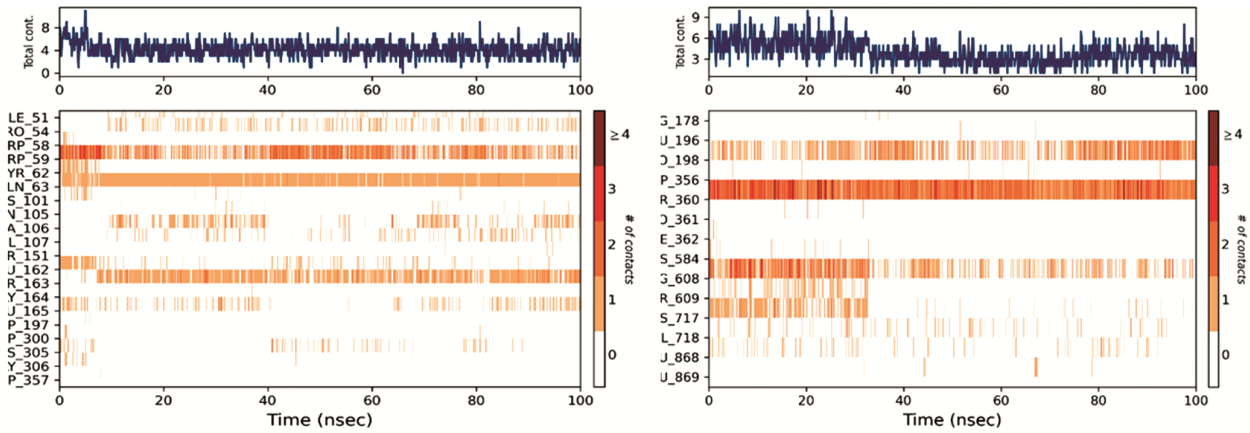

Fig. 8 — Timeline of key protein (PDBID 1B2Y)-ligand (SM-04) & (PDBID 5KZW)-ligand (SM-04) interactions across the simulation trajectory

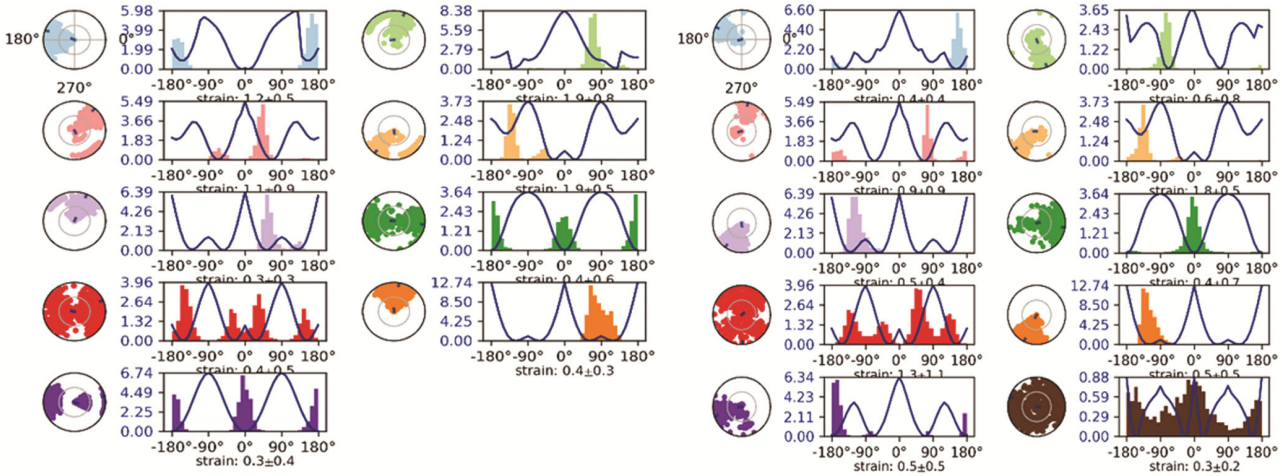

Fig. 9 — Ligand torsion angle profiles of 1B2Y & 5KZW

Table 3— MD Simulation summary metrics (RMSD, Radius of gyration, SASA, MolSA, PSA)

Property	1b2y_SM-04 Complex	5kzw_SM-04 Complex
Ligand RMSD (Å)	Stable	Stable
Radius of Gyration	Consistent	Consistent
MolSA (Å²)	Within the expected range	Within the expected range
SASA (Å²)	Stable	Stable
PSA (Å²)	Minimal fluctuation	Minimal fluctuation

simulations. For the SM-04_1B2Y complex (left), most residues exhibited fluctuations below 1.2 Å, with minor peaks around residue indices ~50, ~300, and ~620, and the highest flexibility (~2.9 Å) observed near the terminal and loop regions, which are generally less structurally constrained. Similarly, in the SM-04_5KZW complex (right), fluctuations remained predominantly below 1.0 Å for the majority of residues, with slightly higher peaks (~2.8 Å) observed in terminal and loop segments around residue indices ~50, ~280, and ~620. Active-site residues (highlighted in green) showed minimal deviation (<0.8 Å), confirming their structural stability and supporting persistent ligand binding throughout the simulation. These results suggest that SM-04 binding did not induce significant conformational changes in either α-glucosidase or α-amylase, maintaining the integrity of the catalytic pocket.

Both systems displayed stable ligand RMSD values, consistent radius of gyration, and minimal fluctuations in solvent-accessible surface area (SASA) and polar surface area (PSA). Molecular surface area (MolSA) remained within the expected range, indicating no significant structural collapse. Hydrogen bonding interactions were maintained throughout the trajectory, confirming stable ligand–protein associations (Figs. 6-9, and Table 3).

***In vitro* study**

MTT assay for cytotoxicity and protective effect

MTT assay was employed to evaluate both the cytotoxic potential and the protective effect of all synthesised compounds in 3T3-L1 fibroblasts under hyperglycemic stress (200 mg/dL glucose). At concentrations ranging from 20–100 µg/mL, all test compounds exhibited higher cell viability compared to the standard α-glucosidase inhibitor acarbose. The IC_{50} values for cytotoxicity were >80 µg/mL for most compounds, indicating low intrinsic cytotoxicity. Among the series, SM-01, SM-03, SM-05, and SM-06 showed slightly lower IC_{50} values (~87–90 µg/mL), while SM-02 and SM-04 did not reach 50% inhibition at the tested concentrations. The results obtained are shown in (Table 4).

Table 4 — Cytotoxic effects of compound against 3T3 L1 Cell lines

S. No	Sample Code	Conc.	OD			Mean	% Inhibition	% viability	IC_{50} (g/mL)
1	Control			1.534		-	-	-	-
		20	0.977	0.975	0.979	0.977	36.31%	63.69%	
2	Standard	40	0.756	0.744	0.748	0.746	51.36%	48.64%	38.12
	Acarbose	60	0.519	0.521	0.518	0.519	66.19%	33.84%	
		80	0.389	0.389	0.387	0.388	74.70%	25.3%	
		100	0.246	0.248	0.244	0.246	83.96%	16.04%	
		20	1.421	1.425	1.423	1.423	7.23%	92.77%	
3	SM-01	40	1.309	1.313	1.308	1.310	14.59%	85.41%	89.45
		60	1.085	1.091	1.089	1.088	29.09%	70.91%	
		80	0.844	0.849	0.843	0.845	44.90%	55.10%	
		100	0.628	0.635	0.631	0.631	58.85%	41.15%	
		20	1.467	1.460	1.462	1.463	4.63%	95.37%	
4	SM-02	40	1.153	1.156	1.151	1.153	24.86%	75.14%	>100 (NE)
		60	1.000	0.996	0.998	0.998	34.91%	65.09%	
		80	0.950	0.945	0.948	0.948	38.20%	61.80%	
		100	0.837	0.840	0.836	0.838	45.37%	54.63%	
		20	1.427	1.426	1.426	1.426	7.04%	92.96%	
5	SM-03	40	1.312	1.314	1.311	1.312	14.47%	85.53%	88.38
		60	1.103	1.106	1.081	1.096	28.55%	71.45%	
		80	0.841	0.843	0.847	0.844	44.98%	55.02%	
		100	0.634	0.637	0.639	0.637	58.47%	41.53%	
		20	1.462	1.464	1.461	1.463	4.62%	95.38%	
6	SM-04	40	1.168	1.171	1.166	1.168	23.85%	76.15%	NE
		60	0.991	0.992	0.990	0.991	35.39%	64.61%	
		80	0.950	0.956	0.953	0.953	37.87%	62.13%	
		100	0.850	0.846	0.846	0.854	44.32%	55.68%	
		20	1.426	1.428	1.425	1.426	7.04%	92.96%	
7	SM-05	40	1.298	1.301	1.299	1.299	15.29%	84.71%	87.25
		60	1.097	1.099	1.094	1.097	28.47%	71.53%	
		80	0.868	0.872	0.870	0.870	43.28%	56.72%	
		100	0.649	0.651	0.648	0.649	57.70%	42.30%	
		20	1.470	1.471	1.473	1.471	4.10%	95.90%	
8	SM-06	40	1.260	1.263	1.259	1.261	17.77%	82.23%	90.12
		60	1.098	1.094	1.096	1.096	28.55%	71.45%	
		80	0.880	0.885	0.882	0.882	42.50%	57.50%	
		100	0.670	0.668	0.669	0.669	56.38%	43.62%	
		20	1.450	1.448	1.452	1.450	5.47%	94.53%	
9	SM-07	40	1.270	1.268	1.273	1.270	17.21%	82.79%	92.34
		60	1.049	1.046	1.048	1.048	31.66%	68.34%	
		80	0.860	0.857	0.859	0.859	43.99%	56.01%	
		100	0.680	0.683	0.681	0.681	55.60%	44.40%	
		20	1.472	1.471	1.469	1.471	4.10%	95.90%	
10	SM-08	40	1.319	1.315	1.317	1.317	14.14%	85.86%	91.87
		60	1.101	1.100	1.103	1.101	28.22%	71.78%	
		80	0.872	0.875	0.870	0.872	43.17%	56.83%	
		100	0.661	0.659	0.663	0.661	56.91%	43.09%	

Table 5— α-amylase enzyme inhibition assay of the derivatives (SM01-08)

S. No	Sample code	Concentration (µg/ml)	α-amylase enzyme inhibition assay					IC50 (µg/ml)
			Absorbance at 540 nm				% Inhibition	
			Test 1	Test 2	Test3	Mean		
1	Control		1.74	1.74	1.74	1.74	-	
		20	1.42	1.45	1.40	1.42	18.39%	
2	Standard (Acarbose)	40	1.07	1.09	1.05	1.07	38.50%	48.13
		60	0.71	0.74	0.69	0.71	59.19%	
		80	0.50	0.53	0.48	0.50	71.26%	
		100	0.29	0.28	0.25	0.27	84.48%	
		20	1.5	1.49	1.51	1.5	13.79%	
3	SM-01	40	1.45	1.47	1.46	1.46	16.09%	92.85
		60	1.34	1.33	1.35	1.34	22.99%	
		80	1.19	1.18	1.18	1.18	32.18%	
		100	1.06	1.03	1.05	1.05	39.66%	
		20	1.41	1.39	1.39	1.4	19.54%	
4	SM-02	40	1.3	1.31	1.31	1.31	24.71%	90.96
		60	1.12	1.11	1.11	1.11	36.21%	
		80	1.01	1.01	1.0	1.01	41.95%	
		100	0.87	0.87	0.86	0.87	50.0%	
		20	1.68	1.66	1.65	1.66	4.59%	
5	SM-03	40	1.45	1.44	1.47	1.45	16.66%	98.28
		60	1.10	1.13	1.08	1.10	36.78%	
		80	0.91	0.94	0.88	0.91	47.70%	
		100	0.82	0.86	0.84	0.84	51.72%	
		20	1.70	1.72	1.67	1.69	2.87%	
6	SM-04	40	1.48	1.46	1.51	1.48	14.94%	81.71
		60	0.91	0.93	0.88	0.90	48.27%	
		80	0.82	0.82	0.85	0.83	52.29%	
		100	0.71	0.72	0.71	0.71	59.19%	
		20	1.33	1.32	1.31	1.32	24.14%	
7	SM-05	40	1.13	1.12	1.13	1.13	35.06%	73.07
		60	1.07	1.09	1.08	1.08	37.93%	
		80	0.78	0.8	0.8	0.79	54.6%	
		100	0.58	0.61	0.59	0.59	66.09%	
		20	1.24	1.22	1.22	1.23	29.31%	
8	SM-06	40	1.01	1.03	1.03	1.02	41.38%	76.75
		60	0.83	0.84	0.83	0.83	52.3%	
		80	0.72	0.73	0.75	0.73	58.05%	
		100	0.47	0.48	0.47	0.47	72.99%	
		20	1.45	1.46	1.47	1.46	16.09%	
9	SM-07	40	1.28	1.26	1.28	1.27	27.01%	98.63
		60	1.3	1.3	1.28	1.29	25.86%	
		80	1.01	1.0	1.01	1.01	41.95%	
		100	0.86	0.85	0.86	0.86	50.57%	
		20	1.3	1.29	1.31	1.3	25.29%	
10	SM-08	40	1.09	1.06	1.06	1.07	38.51%	78.46
		60	0.96	0.96	0.95	0.96	44.83%	
		80	0.8	0.78	0.79	0.79	54.6%	
		100	0.57	0.56	0.57	0.57	67.24%	

α-amylase enzyme inhibition assay

The α-amylase inhibition activity of SM-01 to SM-08 was assessed using the Bernfeld method (20–100 µg/mL) with acarbose as a standard. An IC_{50} values for the synthesized compounds ranged from 73.07 µg/mL (SM-05) to 98.63 µg/mL (SM-07), compared to 48.13 µg/mL for acarbose. SM-05, SM-06, and SM-08 exhibited the highest inhibitory activity, with >65% inhibition at 100 µg/mL. SM-02, SM-04, and SM-07 showed moderate inhibition, while SM-01 and SM-03 were comparatively weaker inhibitors. The results obtained are shown in the (Table 5).

Discussion

All synthesized compounds (SM-01 to SM-08) were analyzed and structurally confirmed by melting point MP, ^{1}H NMR, ^{13}C NMR, and mass spectrometry, ensuring the integrity and purity of the chemical entities prior to biological and computational evaluation. The integrated *in silico*, *in vitro*, and ADMET profiling provided a comprehensive assessment of their potential as dual α-glucosidase and α-amylase inhibitors for managing postprandial hyperglycemia.

Docking analysis revealed that the synthesized ligands displayed considerable binding affinity toward both α-glucosidase and α-amylase, positioning them as potential dual inhibitors. While acarbose exhibited the highest binding energy, several SM-series compounds approached its docking performance, indicating strong lead potential. In α-glucosidase, key residues such as TRP357, THR163, and GLY306 were recurrently involved in van der Waals and π–π stacking interactions, particularly TRP357, which stabilized aromatic scaffolds. Notably, SM-06 and SM-08, despite similar docking scores, differed in their interaction patterns, suggesting possible variation in dynamic stability and inhibitory efficacy.For α-amylase, high-affinity ligands (SM-02, SM-04, SM-06, SM-08) interacted predominantly with GLY359, TYR609, and ARG585—residues critical for carbohydrate recognition and catalysis. SM-04's interaction with TYR609 conferred additional π–π stabilization, whereas SM-02 and SM-08 engaged ARG585, likely contributing to electrostatic stabilization and competitive inhibition. Across both targets, the ligands maintained consistent aromatic and hydrogen-bond interactions in hydrophobic pockets, closely mirroring reported inhibitor–enzyme complexes.

Building on the docking results, ADMET profiling provided additional insight into the drug-likeness of the SM-series and helped to differentiate them from acarbose. The synthesized molecules demonstrated higher lipophilicity (logP 5.68–6.98), favorable for hydrophobic pocket occupancy, but potentially limiting aqueous solubility. Despite this, most compounds showed high predicted gastrointestinal absorption, aided by an optimal hydrogen-bond donor/acceptor balance. SM-06, with the highest logP and molecular weight, exhibited lower GI absorption. None of the compounds crossed the blood–brain barrier, an advantage for non-CNS-targeting antidiabetic agents. Bioavailability scores were moderate (0.17–0.55), suggesting that formulation strategies may further improve systemic exposure. All compounds exhibited low hepatotoxicity and nephrotoxicity risk, supporting favorable safety potential.

The stability of binding interactions was further validated through molecular dynamics simulations. MD simulations for SM-04 complexes with α-glucosidase (PDB ID: 1B2Y) and α-amylase (PDB ID: 5KZW) demonstrated stable ligand RMSD profiles, indicating early and sustained accommodation within the active site. The radius of gyration remained consistent, implying no destabilizing conformational changes to the proteins. Stable SASA and MolSA values confirmed a compact ligand–protein interface, while minimal PSA fluctuations reflected persistent hydrogen-bond networks particularly with GLY359 and TYR609 in 5KZW. The persistence of both hydrogen bonds and hydrophobic contacts reinforced SM-04's predicted high-affinity dual inhibitory capacity.

MTT assays on fibroblast cells demonstrated that all compounds maintained >70% cell viability at ≤60 μg/mL, indicating low cytotoxic potential. SM-02 and SM-04 were particularly well tolerated, with no IC_{50} reached at the highest tested concentration (100 μg/mL), while other analogs exhibited IC_{50} values between 87–92 μg/mL—still well above predicted therapeutic ranges. Compared to acarbose ($IC_{50} \approx 38$ μg/mL), the SM-series showed significantly lower cytotoxicity, suggesting reduced off-target toxicity.

Enzyme inhibition assays indicated that SM-05 (IC_{50}: 73.07 μg/mL) and SM-06 (IC_{50}: 76.75 μg/mL) were the most potent α-amylase inhibitors, achieving >65% inhibition at 100 μg/mL. While SM-02 and SM-04 showed only moderate inhibition in this assay, their strong docking scores and MD stability suggest potential synergistic efficacy via dual α-amylase/α-glucosidase inhibition. SAR indicated that increased hydrogen-bonding potential and hydrophobic interactions correlated with higher activity, while steric hindrance and suboptimal electronic distribution reduced potency in some analogs. Anita Azmi *et al*., developed imidazole-bearing thioquinoline hybrids and evaluated their α-glucosidase inhibitory activity using *in vitro* assays, docking, MD simulation, and *in vivo* evaluation in diabetic rat models. Lead compound 8g (Fig. 10) exhibited remarkably low IC_{50} (~12.1 μM) compared to acarbose (~750 μM),

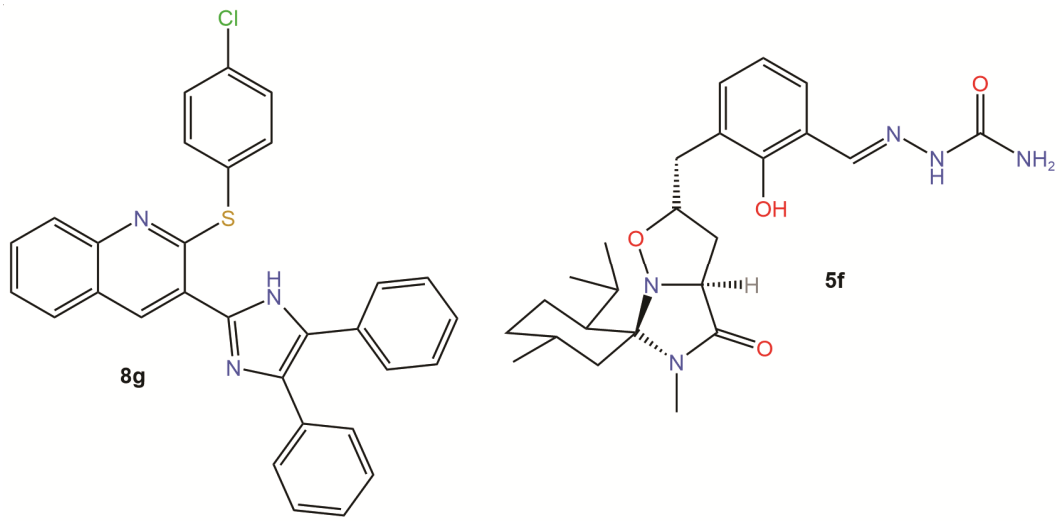

Fig. 10 — Previously reported synthesized compounds which are significant α-amylase and α-glucosidase inhibitors

demonstrated stable enzyme binding, and significantly reduced fasting and postprandial glucose in animal studies without acute toxicity. This offers a significant translational precedent demonstrating how imidazole-modified scaffolds can progress from computational validation to biological efficacy *in vivo*[24].

From a medicinal chemistry perspective, the collective data highlight SM-02, SM-04, SM-05, SM-06, and SM-08 as priority scaffolds for optimization. SM-02 and SM-04 are attractive for their exceptional safety margins and dynamic stability, while SM-05 and SM-06 offer stronger α-amylase inhibition. Al Rashidi *et al.*[25], reported the enzyme inhibition potency of imidazo-isoxazole derivatives targeting both α-amylase and α-glucosidase. Their most active compounds5f (Fig. 10) showed inhibitory potency (IC_{50} of α-amylase and α-glucosidase is 26.67 ±1.25 µM and 39.12 ±1.83 µM, respectively) superior to acarbose, and comprehensive validation was conducted via enzymatic assays, docking, and multiscale MD simulations. This study closely parallels our approach using similar heterocyclic scaffolds and a dual-target strategy affirming the robustness of imidazole-based antidiabetic agents. The balance between computational affinity, ADMET favorability, *in vitro* stability, and low cytotoxicity supports the SM-series as promising candidates for further lead development in dual-target postprandial glycemic control.

Conclusion

The present study successfully integrates computational, synthetic, and biological approaches to identify novel imidazole-based derivatives with significant antidiabetic potential. The designed compounds demonstrated favorable binding affinities toward α-amylase and α-glucosidase, supported by stable protein–ligand interactions during molecular dynamics simulations. ADMET profiling further reinforced their drug-likeness, while *in vitro* assays confirmed potent α-amylase inhibition, with compound SM-04 exhibiting activity comparable to the reference drug acarbose. Collectively, these findings underscore the imidazole scaffold as a promising pharmacophore for T2DM management and justify advancing these derivatives into further preclinical and mechanistic studies to establish their therapeutic applicability.

Future Prospect

Building on the promising *in silico* and *in vitro* outcomes of the synthesized imidazole derivatives, future work should focus on *in vivo* pharmacodynamic and pharmacokinetic evaluations to establish their efficacy and safety profiles in biological systems. Structural optimization, guided by SAR insights, could further enhance potency, selectivity, and metabolic stability. Mechanistic studies to elucidate the precise molecular pathways involved in glucose regulation will deepen our understanding of their therapeutic action. Additionally, evaluating these derivatives against other diabetes-related targets, such as DPP-4 or PPAR-γ, could expand their potential as multi-target antidiabetic agents. Integration of nanocarrier-based delivery systems may also be explored to overcome solubility limitations and improve bioavailability, ultimately paving the way for clinical translation.

Acknowledgement

We thank the Department of Pharmaceutical Chemistry, BLDEA's Shri Sanganabasava Mahaswamiji College of Pharmacy and Research Centre, Vijayapur, Karnataka, for providing all the required things used in this research.

Conflict of interest

All authors declare no conflict of interest.

References

1 Siam NH, Snigdha NN, Tabasumma N & Parvin I, Diabetes Mellitus and Cardiovascular Disease: exploring epidemiology, pathophysiology, and treatment strategies. *Rev Cardiovasc Med* 25 (2024) 436.

2 Hossain MJ, Al-Mamun M & Islam MR, Diabetes mellitus, the fastest growing global public health concern: Early detection should be focused. *Health Sci Rep*, 7 (2024) e2004.

3 Association AD, Standards of medical care in diabetes—2011. *Diabetes Care*, 34 (2011) S11.

4 Sun H, Saeedi P, Karuranga S, Pinkepank M, Ogurtsova K, Duncan BB, Stein C, Basit A, Chan JCN & Mbanya JC, IDF Diabetes Atlas: Global, regional and country-level diabetes prevalence estimates for 2021 and projections for 2045. *Diabetes Res Clin Pract*, 183 (2022) 109119.

5 Lerman I, Adherence to treatment: the key for avoiding long-term complications of diabetes. *Arch Med Res*, 36 (2005) 300.

6 Shukla PK, Verma A & Mishra P, Significance of nitrogen heterocyclic nuclei in the search of pharmacological active compounds. *New perspective in agricultural and human health*, 100 (2017).

7 Abdella AM, Abdelmoniem AM, Abdelhamid IA & Elwahy AHM, Synthesis of heterocyclic compounds via Michael and Hantzsch reactions. *J Heterocycl Chem*, 57 (2020) 1476.

8 Welsch ME, Snyder SA & Stockwell BR, Privileged scaffolds for library design and drug discovery. *Curr Opin Chem Biol,* 14 (2010) 347.

9 Lohitha N & Vijayakumar V, Imidazole appended novel phenoxyquinolines as new inhibitors of α-amylase and α-glucosidase evidenced with molecular docking studies. *Polycycl Aromat Compd,* 42 (2022) 5521.

10 Alagesan K, Raghupathi PK & Sankarnarayanan S, Amylase inhibitors: potential source of anti-diabetic drug discovery from medicinal plants. *Int J Pharm Life Sci,* 3 (2012) 1407.

11 Hollingsworth SA & Dror RO, Molecular dynamics simulation for all. *Neuron*, 99 (2018) 1129.

12 Siddiqui B, Yadav CS, Akil M, Faiyyaz M, Khan AR, Ahmad N, Hassan F, Azad MI, Owais M & Nasibullah M, Artificial intelligence in computer-aided drug design (cadd) tools for the finding of potent biologically active small molecules: Traditional to modern approach. *Comb Chem High Throughput Screen* (2025).

13 Badar MS, Shamsi S, Ahmed J & Alam MA, Molecular dynamics simulations: concept, methods, and applications. Molecular dynamics simulations: concept, methods, and applications. *Springer*, 5 (2022) 131.

14 Riyaphan J, Pham DC, Leong MK & Weng CF, *In silico* approaches to identify polyphenol compounds as α-glucosidase and α-amylase inhibitors against type-II diabetes. *Biomolecules*, 11 (2021) 1877.

15 Zala SP, Badmanaban R, Sen DJ & Patel CN, Synthesis and biological evaluation of 2, 4, 5-triphenyl-1H-imidazole-1-yl Derivatives. *J Appl Pharm Sci*, 2 (2012) 202.

16 Metri SM, Synthesis and Biological Evaluation of Some New 1, 3, 4-Oxadiazole Derivatives. (2016).

17 Alp M, Misturini A,&Sastre G, Computational design of new drugs for binding-amylase as candidates for treating diabetes. (2022) 1.

18 Kurmi SPC, Thapa S, Mahmood AAR, Murav AK, Biradar MS, Bhagyanath N& Maurya SN, Medicinal chemistry insights of molecular docking and cell permeability mechanism of phytoconstituents present in Mimosa pudica as NS2B-NS3 protease inhibitors against dengue virus. *Discov Chem*, 2 (2025) 78.

19 Shivakumar D, Williams J, Wu Y, Damm W, Shelley J & Sherman W, Prediction of absolute solvation free energies using molecular dynamics free energy perturbation and the OPLS force field. *J Chem Theory Comput*, 6 (2010) 1509.

20 Thapa S, Maurya SN, Manjunath K, Mahmood AA, Devi K, Varghese SA, Lamsal A, Tamang B & Biradar MS, LC-MS profiling and multi-target mechanistic insights of Hibiscus rosa-sinensis in diabetes: Network pharmacology, molecular docking, MD simulation, PCA, and *in vitro* α-amylase inhibition. *Pharmacol Res Mod Chin Med*, 16 (2025) 100636.

21 Kiran S, Javid S, Metri SM, Kurmi SPC, Hemavathi S, Murav AK, Biradar MS & Thapa S, Integrated computational approach revealed the potential inhibitory effect of xanthone derivatives against Marburg virus nucleocapsid. *Virusdisease* (2025).

22 Stępnik M, Arkusz J, Smok-Pieniążek A, Bratek-Skicki A, Salvati A, Lynch I, Dawson KA, Gromadzińska J, Jong WH De & Rydzyński K, Cytotoxic effects in 3T3-L1 mouse and WI-38 human fibroblasts following 72 hour and 7-day exposures to commercial silica nanoparticles. *Toxicol Appl Pharmacol*, 263 (2012) 89.

23 Nyambe-Silavwe H, Villa-Rodriguez JA, Ifie I, Holmes M, Aydin E, Jensen JM & Williamson G, Inhibition of human α-amylase by dietary polyphenols. *J Funct Foods*, 19 (2015) 723.

24 Azmi A, Noori M, Ghomi MK, Montazer MN, Iraji A, Dastyafteh N, Oliyaei N, Khoramjouy M, Rezaei Z & Javanshir S, Alpha-glucosidase inhibitory and hypoglycemic effects of imidazole-bearing thioquinoline derivatives with different substituents: *In silico*, *in vitro*, and *in vivo* evaluations. *Bioorg Chem*, 144 (2024) 107106.

25 AlRashidi E, Ghannay S, Albadri AEAE, Abid M, Kadri A & Aouadi K, Design, synthesis, biological evaluation, kinetic studies and molecular modeling of imidazo-isoxazole derivatives targeting both α-amylase and α-glucosidase inhibitors. *Heliyon*, 10 (2024).